WATER RESOURCES RESEARCH, VOL. 49, 1741–1745, doi:10.1002/wrcr.20144, 2013

Capabilities and limitations of tracing spatial temperature patterns by fiber-optic distributed temperature sensing

Liliana Rose,[1] Stefan Krause,[1] and Nigel J. Cassidy[2]

Received 13 September 2012; revised 8 February 2013; accepted 9 February 2013; published 29 March 2013.

[1] Increasing numbers in interdisciplinary applications of Fiber-optic Distributed Temperature Sensing (FO-DTS) call for a quantitative assessment of the limitations and uncertainties of this new technology. This study conducts controlled laboratory experiments to analyze the qualitative (signal size and location) and quantitative (signal intensity) accuracies of FO-DTS surveys of temperature signals higher and lower than ambient temperature, ranging from well above to critically below the FO-DTS sampling interval. Our results reveal that qualitative and quantitative accuracies of FO-DTS measured temperatures critically decline with decreasing signal size, in particular for signals near the spatial sampling interval. Decreasing detection accuracy risks the masking of real temperature variation in highly dynamic systems. The resulting potential ambiguity of interpretations of signal size, intensity, and absolute location will have to be considered in future experimental design and interpretation of FO-DTS surveys.

Citation: Rose, L., S. Krause, and N. J. Cassidy (2013), Capabilities and limitations of tracing spatial temperature patterns by fiber-optic distributed temperature sensing, *Water Resour. Res.*, *49*, 1741–1745, doi:10.1002/wrcr.20144.

1. Introduction

[2] The necessity of precise temperature measurements at scales >100 m and with high-spatial and temporal resolution has triggered the development of new effective sensor technologies including Fiber-optic Distributed Temperature Sensing (FO-DTS). FO-DTS allows for continuous monitoring of spatially distributed temperatures along fiber-optic cables with spatial resolutions of <1 m and accuracies of 0.05°C–0.1°C [*Selker et al.,* 2006a, 2006b; *Hausner et al.,* 2011; *van de Giessen et al.,* 2012]. The spatial resolution of FO-DTS sampled data is limited by the instruments detection capabilities of the laser backscatter [*Tyler et al.,* 2009]. Recent studies of calibration strategies and sampling design for single-ended and double-ended monitoring modes provided benchmark references for FO-DTS applications and improved the understanding of methodological uncertainties and limitations [*Hausner et al.,* 2011; *van de Giessen et al.,* 2012].

[3] Temperature changes along the fiber-optic cable can be rather gradual over larger scales or discrete at small scales. Increasing numbers of FO-DTS applications with different monitoring demands require a precise quantitative understanding of the impacts of the intensity of the temperature signal and signal size (the spatial extent of the temperature signal) on the accuracies and limitations of FO-DTS surveys. The impact of signal size and signal intensity on the actual observation cannot be interpreted independently of each other. Hence, current limitations in understanding signal size dependent uncertainties of FO-DTS observations and related ambiguity in the interpretation of the actual signal intensity impose a risk of inaccurate interpretation and quantitative analysis of temperature patterns.

[4] In order to improve the quantitative understanding of critical uncertainties, this study investigates the signal size dependent accuracy of FO-DTS monitored temperatures. It therefore conducts controlled laboratory experiments and analyzes the qualitative (signal size and location) and quantitative (signal intensity) limitations in FO-DTS monitoring for signal sizes ranging from well above to critically below the FO-DTS sampling interval.

2. Materials and Methods

[5] FO-DTS is based on the analysis of the temperature-dependent Raman spectra backscatter properties of a laser pulse that is applied to and propagates through a fiber-optic cable. It analyzes the Stokes/anti-Stokes power ratio, in combination with travel-time information of the propagating laser pulse in order to quantify temperatures for spatial integration intervals along the fiber-optic cable [*Selker et al.,* 2006a, 2006b; *Hausener et al*., 2011; *van de Giesen et al*., 2012]. The precision of fiber-optic temperature measurements is controlled by the total number of photons detected as a function of integration time and the spatial integration length.

[6] This study applied a Sensornet Halo FO-DTS (Elstree, UK) which analyzed the backscatter properties of a 20 ns light pulse for monitoring temperatures along a 300 m long nonarmoured *BruOutdoo*r dual-fiber cable (Brugg/CH). The spatial averaging at the Halo FO-DTS occurs over 2 m sampling intervals [*Sensornet,* 2009], which is assumed to

[1]School of Geography, Earth and Environmental Sciences, University of Birmingham, Birmingham, Edgbaston, UK.
[2]Department for Geography, Geology and the Environment, Keele University, Keele, Staffordshire, UK.

Corresponding author: S. Krause, School of Geography, Earth and Environmental Sciences, University of Birmingham, Birmingham, Edgbaston B15 2TT, UK. (s.krause@bham.ac.uk)

©2013. American Geophysical Union. All Rights Reserved.
0043-1397/13/10.1002/wrcr.20144

provide a > 4 m monitoring resolution [*van de Giessen et al*., 2012]. To support comparability with other systems, length units were given as multiples of sampling intervals.

[7] FO-DTS surveys were conducted in single-ended mode with the application of the laser pulse and detection of its backscatter from one end of the fiber (Figure 1A). The application of FO-DTS requires calibration involving reference temperature baths and respective adjustment of signal losses which are causing drift along the fiber-optic cable as well as corrections of temperature off-sets [*Tyler et al.,* 2009; *Hausner et al.,* 2011]. With regard to the placement of calibration reference sections, this study deployed a duplex single-ended configuration [*Hausner et al.,* 2011] with reference measurements in constant temperature ice baths at two 20 m long cable sections at both ends of the 300 m long fiber-optic cable (Figure 1) which were matched at fixed temperatures. Ice bath temperatures were recorded by independent thermistor measurements throughout the experiment.

[8] FO-DTS temperature measurements were carried out in cold baths with lower than and warm baths with higher than ambient air temperature. Cold baths were kept at constant temperature, similar to the calibration ice baths. Warm baths were kept at temperature between 40°C and 44°C, using a thermistor controlled heating element and

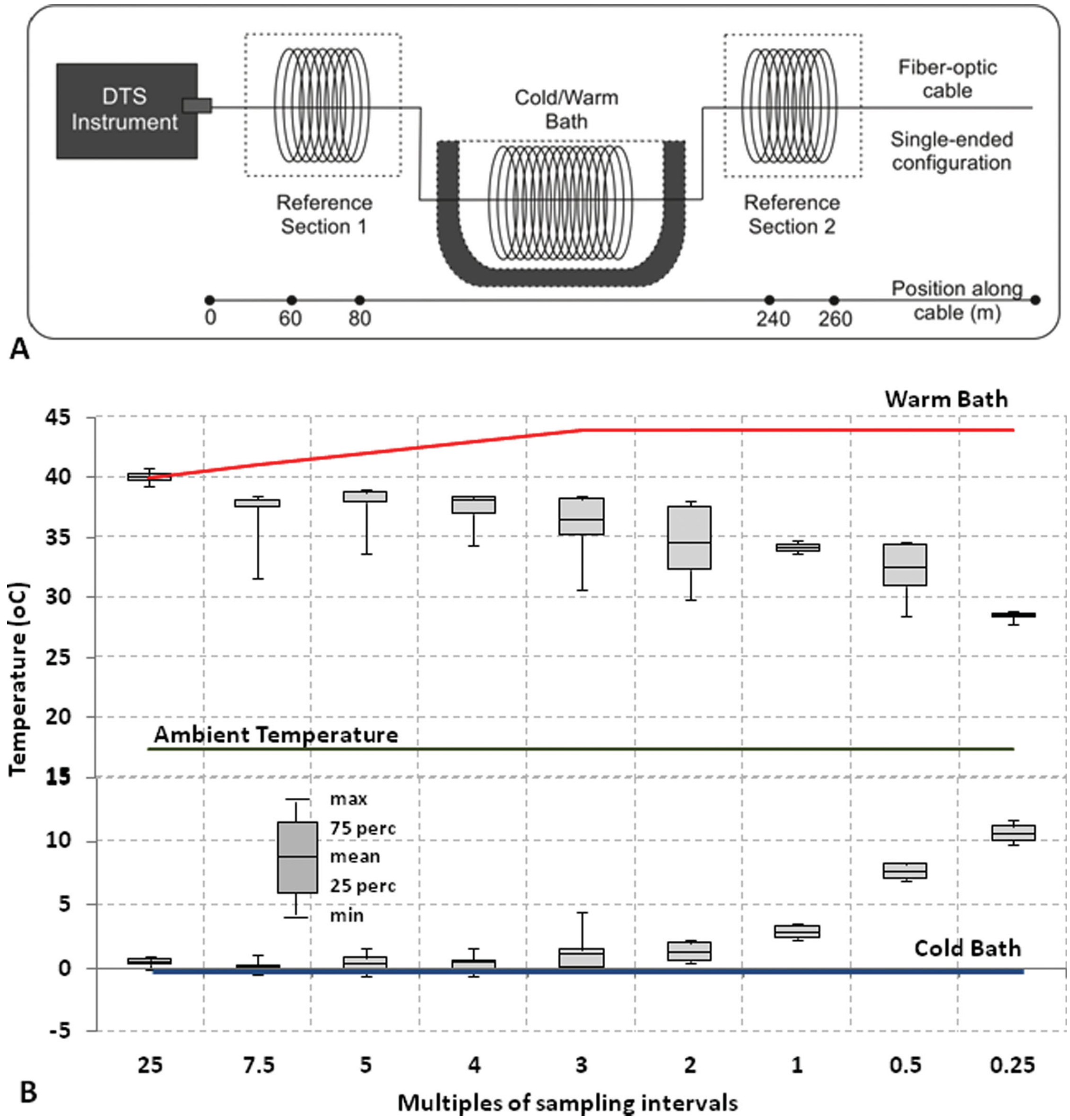

Figure 1. (A) Sampling configuration in single-ended mode with two 20 m temperature reference sections in ice baths of 0°C and a cold or warm baths of variable length (for monitoring sections <20m length two warm or cold baths were applied in line with at least 20 m distance in between); (B) Signal size dependent divergence of FO-DTS observed temperatures (spatially averaged over sampling section) from independent thermistor measurements for two signal strengths of (bottom) 0°C and (top) 40–44°C. Box plots indicate the temporal dispersion of measurements within the same sampling section over a 10 min sampling interval.

circulation pump. The cold-bath and warm-bath temperatures allowed an analysis of the detection accuracy of different signal sizes for temperature anomalies above and below ambient thermal conditions.

[9] Temperatures in the test baths were measured at cable sections from 0.5 (1/4 × sampling interval) to 50 m (25 × sampling interval, Table 1). For the experiments, the respective length sections of fiber-optic cable were led through the reference ice bath before it passes through the test bath and then back through the reference ice bath (Figure 1A). In order to avoid preferential longitudinal heat transport along the cable, a distance of at least at 50 m was ensured between reference baths and the measurement section (Figure 1A). In a subsequent experiment, temperature signals smaller than the sampling interval were analyzed with respect to the impact of their relative location at the cable in order to identify qualitative and quantitative errors in their detection in dependency of the signal interpolation within a sampling interval. Therefore, cable sequences of 2, 1, and 0.5 m (1, 0.5, and 0.25 × sampling interval) were moved stepwise in 1 m (for 1 and 0.5 × sampling interval) and 50 cm (for 0.25 × sampling interval) increments through the warm and cold baths. Cable sections were kept in the cold or warm baths for at least 20 min before measurements commenced in order to allow the cable temperature to equilibrate before collecting data.

[10] Temperatures of nine signal sizes (Table 1) were observed for positive and negative temperature anomalies over 10 min sampling intervals comprising 20 measurements of 30 s duration each. For the analysis of the qualitative and quantitative signal accuracy, FO-DTS results for cable sections in cold and warm baths were compared to independent thermistor reference measurements. For the assessment of signal size dependent sampling accuracy, mean, minimum, and maximum temperatures as well as standard deviations (STDV) and root mean square error (RMSE) were analyzed.

3. Results and Discussion

[11] The accuracy of FO-DTS temperature measurements in the 0°C calibration ice-bath sections was 0.45°C (RMSE), based on 1489 measurements over the course of the experiment with STDEV of 0.09 and 0.15 for the cold and warm anomaly experiments respectively.

[12] Averages (10 min) of FO-DTS observed cold-bath and warm-bath temperatures for signal sizes from 0.25 to 25 times the FO-DTS sampling interval (Table 1) were compared to independent thermistor reference measurements in the temperature baths (Figure 1B). The divergence of FO-DTS temperatures from thermistor reference measurements was <1°C for measurements of cold anomalies with signal sizes of 25–7.5 times the sampling interval (Figure 1B), while differences for smaller signal sizes with only 1–0.25 times the sampling interval exceeded 10°C (Table 1). For warm anomalies FO-DTS absolute errors of <1°C were only seen for signal sizes of 25 times the sampling interval (Figure 1B). FO-DTS monitored temperatures for warm anomalies with signal sizes of 7.5–0.25 times the sampling interval differed by 4.02°C–15.5°C from reference measurements (Table 1). Averaged FO-DTS observed warm-bath temperatures were statistical more dispersed than cold-bath temperatures (Figure 2) as indicated by higher STDV (Table 1), which may result from the fact that the strength of the positive temperature anomaly (23°C–14°C) was higher than of the negative temperature anomaly (~17°C). In addition, warm-bath temperatures deviated more from the calibration temperature than the cold baths. As indicated by the higher absolute error (differences to references measurements 0.22°C to −15.5°C; STDV 0.08–0.38), FO-DTS measurement accuracy was lower for warm baths than for cold baths (absolute error −0.25°C to 11.21°C; STDV 0.08–0.14; Table 1), with a strong dependency of the FO-DTS monitoring accuracy on the actual signal size in both cases (Table 1, Figure 1B).

[13] Reduced sampling accuracy for smaller sized signals was furthermore affected by the increased proportional impact of inaccurate prediction of temperatures at the spatial margins of the signal (Figure 2A). *van de Giessen et al.* [2012] suggest that precise FO-DTS measurements require signal sizes of at least twice the sampling size. As Figure 2A suggests, the required signal size might be even higher due to considerable edge effects caused by inaccurate signal detection at the margins of cold-bath or warm-bath sections. The intensity and relative impact of such edge effects was inversely correlated to the signal size. The shorter the length of the monitored signal, the higher the impact of the observed edge effects as the relative impact on the spatially averaged temperature signal increased (Figure 2A).

Table 1. FO-DTS Monitored (20 Measurements of 30 s Length) and Thermistor Observed Temperatures for Variable Signal Sizes Ranging From 0.25–25 × the Applied FO-DTS Sampling Interval and $\Delta T = T_{\text{FO-DTS}} - T_{\text{Thermistor}}$ for Cold and Warm Baths as Well as FO-DTS Standard Deviations (STDV), all Values in °C, STDV in Calibration Baths were 0.09 and 0.15 for Cold and Warm Anomaly Experiments, Respectively

Multiples of Sampling Interval	Cold Bath				Warm Bath			
	$T_{\text{FO-DTS}}$	$T_{\text{Thermistor}}$	$\text{STDV}_{\text{FO-DTS}}$	ΔT	$T_{\text{FO-DTS}}$	$T_{\text{Thermistor}}$	$\text{STDV}_{\text{FO-DTS}}$	ΔT
0.25	11.21	0.00	0.13	11.21	28.50	44.00	0.12	−15.50
0.5	9.32	0.00	0.10	9.32	30.78	44.00	0.17	−13.22
1	7.63	0.00	0.14	7.63	34.47	44.00	0.20	−9.53
2	0.63	0.00	0.10	0.63	37.81	44.00	0.12	−6.19
3	0.06	0.00	0.12	0.06	38.23	44.00	0.17	−5.77
4	−0.38	0.00	0.08	−0.38	38.41	43.00	0.08	−4.59
5	−0.36	0.00	0.11	−0.36	38.74	42.00	0.18	−3.26
7.5	−0.17	0.00	0.11	−0.17	37.72	41.00	0.38	−3.28
25	−0.25	0.00	0.08	−0.25	40.22	40.00	0.25	0.22

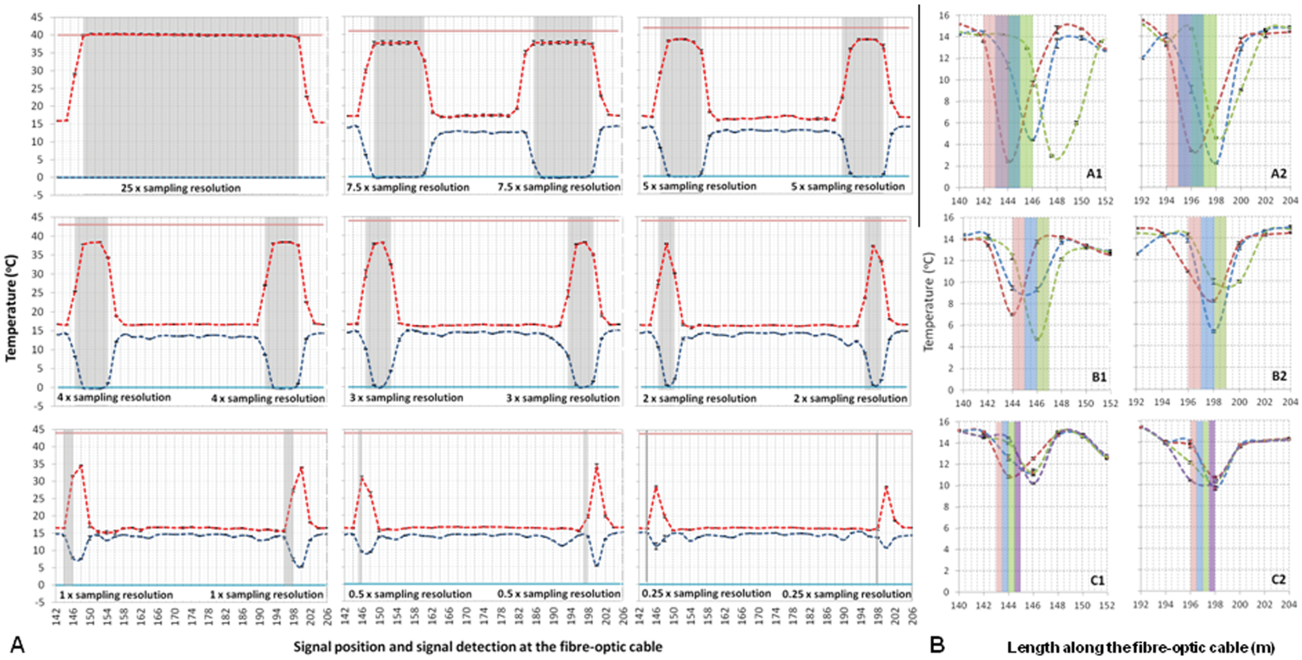

Figure 2. (A) Spatially detailed FO-DTS temperatures for signal sizes between 0.25 and 25 multiples of the sampling interval in comparison to actual signal location and spatial extent; grey bars indicate size and location of the temperature bath with blue and red lines presenting the respective temperatures in the baths; (B) Qualitative (signal size and location) and quantitative (signal strength) limitations of FO-DTS for signal sizes similar or smaller than the sampling interval, with three increments (moved by 0.5 sampling intervals) for signals sizes of 1 (A1, A2), 0.5 × sampling interval (B1, B2) and four increments (moved by 0.25 sampling intervals) for signals sizes of 0.25 × sampling interval (C1, C2). (Notice the overlap for signal sizes of one sampling interval (A1, A2) originates from the shifting in increments of 0.5 sampling intervals).

[14] The implications of observed edge effects varied for the observed cold and warm anomalies. For cold anomalies with a minimum length of twice the sampling interval, at least for one spatial averaging interval the anomaly was detected with an absolute error < 0.25°C. In comparison, warm anomalies were not identified with an absolute error < −3.28°C for any spatial averaging interval if the signal size was less than 25 times the sampling interval (Figure 2). These uncertainties are critical and can have significant impact on the interpretation of small-scale temperature patterns with discrete changes between adjacent monitoring sequences and small signal sizes as for instance in *Selker et al*. [2006a]; *Lowry et al*. [2007]; *Henderson et al*. [2009]; or *Krause et al*. [2012]. Variable accuracy in detected positive and negative temperature anomalies may result from their uneven differences from ambient temperatures (~17°C vs. 23°C–27°C). Future studies will need to establish their relevance for FO-DTS surveys of systems with temporally variable cold or warm signals as for instance seasonally changing directions of temperature differences between groundwater and surface water [*Lowry et al.,* 2007; *Westhoff et al.,* 2007; *Krause et al.,* 2012].

[15] The observed signal size dependent impact of edge effects did not only affect the measured intensity of temperature anomalies but also the identification of absolute signal locations (Figure 2B). For signal sizes below the sampling interval, not only the absolute value and spatial extent of the signal were estimated inaccurately but small variations in the exposed cable section also caused a significant shift in the detected signal location (Figure 2B). The signal size dependent absolute error was 3.42°C, 7.02°C, and over 11.23°C for measurements of signal sizes of 1, 0.5, and 0.25 times the sampling interval. Furthermore, observed temperature signals of sizes of 1, 0.5, and 0.25 times the sampling interval were offset by up to 1–1.5 times of the length of a sampling interval (Figure 2B). Quantitative as well as qualitative inaccuracies of signal detection can have significant implications for the interpretation of FO-DTS surveys. There is a critical risk that locations of signals close to or below the specific FO-DTS sampling interval may be identified incorrectly. The identified inaccuracies of detected signal locations (Figure 2B) were of an extent that can critically interfere with the interpretation of FO-DTS results, in particular when analyzing small-scale thermal patterns as in *Lowry et al*. [2007]; *Henderson et al*. [2009]; *Krause et al*. [2012]; and *Keller et al*. [2011]. Furthermore, interpretations of observations remain ambiguous in particular if the actual signal size is unknown. The impact of the signal size on the observation cannot be distinguished from the impact of the signal intensity (strength of the temperature anomaly). Hence, signals of small size and signals of low intensity may lead to similar observation results that cannot be discriminated from each other. Such ambiguity is of relevance for the interpretation of the steepness and curvature of observed step changes in temperature [e.g. *Selker et al.,* 2006a, 2006b; *Tyler et al.,* 2009] as well as the intensity and spatial extent of small-scale temperature anomalies [*Lowry et al.,* 2007; *Henderson et al.,* 2009; *Krause et al.,* 2012].

4. Conclusions

[16] Comparison of FO-DTS monitoring of warm and cold temperature anomalies of variable spatial extent revealed that qualitative (signal size and location) and quantitative (signal intensity) accuracies of observed temperatures can vary substantially with the spatial extent of the monitored signal, causing variable intensities of signal loss and dislocation. Our results indicate a critical deterioration of quantitative accuracy of FO-DTS measured temperatures with reducing signal size and additionally reduced qualitative accuracy for signal sizes below the spatial sampling interval. The fact that in particular for temperature patterns of small spatial extent the impact of signal intensity and signal size cannot be distinguished sufficiently without additional information can lead to potentially ambiguous interpretations of the size, intensity and absolute location of signals. These inaccuracies have to be considered when critically interpreting FO-DTS surveys of unknown signal sizes and are of particular relevance for the interpretation of surveys with signal sizes below the sampling resolution.

[17] **Acknowledgments.** The authors would like to acknowledge funding for this work by the UK Natural Environment Research Council, NERC (NE/I016120).

References

Hausner, M. B., F. Suárez, K. E. Glander, N. Giesen, J. S. Selker, and S. W. Tyler, (2011), Calibrating single-ended fiber-optic Raman spectra distributed temperature sensing data, *Sensors*, *11*, 10,859–10,879.

Henderson, R. D., F. D. Day-Lewis, and C. F. Harvey (2009), Investigation of aquifer-estuary interaction using wavelet analysis of fiber-optic temperature data, *Geophys. Res. Lett.*, *36*, L06403, doi:10.1029/2008GL036926.

Krause, S., T. Blume, and N. J. Cassidy (2012), Investigating patterns and controls of groundwater up-welling in a lowland river by combining fibre-optic distributed temperature sensing with observations of vertical head gradients, *Hydrol. Earth Syst. Sci. Discuss.*, *9*, 337–378.

Keller, C. A., H. Huwald, M. K. Vollmer, A. Wenger, M. Hill, M. B. Parlange, and S. Reinman (2011), Fiber optic distributed temperature sensing for the determination of the nocturnal atmospheric boundary layer height, *Atmos. Meas. Tech.*, *4*, 143–149.

Lowry, C. S., J. F. Walker, R. J. Hunt, and M. P. Anderson (2007), Identifying spatial variability of groundwater discharge in a wetland stream using a distributed temperature sensor, *Water Resour. Res.*, *43*, W10408, doi:10.1029/2007WR006145.

Selker, J. S., L. Thévanaz, H. Huwald, A. Mallet, W. Luxemburg, N. van de Giesen, M. Stejskal, J. Zeman, M. C. Westhoff, and M. B. Parlange (2006a), Distributed fiber-optic temperature sensing for hydrologic systems, *Water Resour. Res.*, *42*, W12202, doi:10.1029/2006WR005326.

Selker, J. S., N. C. van de Giesen, M. Westhoff, W. Luxemburg, and M. Parlange (2006b), Fiber-optics opens window on stream dynamics, *Geophys. Res. Lett.*, *33*, L24401, doi:10.1029/2006GL027979.

Sensornet 2009, *Sentinal DTS User Guide SEN2-UM1.0*, Sensornet Ltd., London, UK.

Tyler, S. W., J. S. Selker, M. B. Hausner, C. E. Hatch, T. Torgersen, C. E. Thodal, and S. G. Schladow (2009), Environmental temperature sensing using Raman spectra DTS fiber-optic methods, *Water Resour. Res.*, *45*, W00D23, doi:10.1029/2008WR007052.

van de Giesen, N., S. C. Steele-Dunne, J. Jansen, O. Hoes, M. B. Hausner, S. Tyler, and J. Selker (2012), Double-ended calibration of fiber-optic Raman spectra distributed temperature sensing data, *Sensors*, *12*(5), 5471–5485.

Westhoff, M. C., H. H. G. Savenije, W. M. J. Luxemburg, G. S. Stelling, N. C. van de Giesen, J. S. Selker, L. Pfister, and S. Uhlenbrook (2007), A distributed stream temperature model using high resolution temperature observations, *Hydrol. Earth Syst. Sci.*, *11*(4), 1469–1480.